

# FAILURE PHENOMENA IN HYDRODYNAMIC BEARING

Jai Prakash sharma<sup>1</sup>, M R Tyagi<sup>1</sup>, G D Thakre<sup>2</sup>

<sup>1</sup>Department of Mechanical Engineering, Manav Rachna University, Faridabad, India

<sup>2</sup>Tribology & Combustion Division, CSIR-Indian Institute of Petroleum, Dehradun, India

## Abstract

The purpose of this paper is to present a brief on the development of cavitation in Hydrodynamic bearing (HDB) that help design engineer for proper selection of design parameter i.e. L/D ratio, speed and relative clearance. CFD analysis was performed to study the cavitation phenomena causing failure of HDB. It was found that with an increase in speed and L/D ratio, cavitation occurs at an early stage with respect to low speed and lower L/D ratio. Greater importance should be provided for higher load carrying capacity through pressurised fluid supply to prevent cavitation.

**Keywords:** Hydrodynamic lubrication, journal bearing, cavitation, CFD analysis

## 1.0 Introduction

Cavitation occurred as the pressure falls below atmospheric pressure when the surface move apart in the divergent region releasing the dissolved gases within the lubricant[1]. Due to cavitation, metal to metal contact occur causing material loss, noise, vibration etc.[2]. The possible reason behind occurrence of cavitation due to fluctuation in load, speed, variation in fluid properties, friction etc. [3]. This can be minimised through use of lubricant feed pressure. Also large lubricant supply grooves are used to do the same[4]. The recognized form of cavitation is Gaseous, Pseudo cavitation and vapour cavitation discussed in literatures[5]

Reynolds's identified the influence of cavitation due to formation of cavities resulting in pressure disturbance adversely affecting load carrying capacity. As formation of bubbles due to cavitation, film rupture exists in the continuity of the liquid film which is not fulfilled by Reynolds's equation. Sommerfeld [6] solved for 360° full film oil clearance journal bearing which allowed for sub atmospheric and even negative pressure with lower values[7] in Cavitation and related phenomena in lubrication[5]. Gumbel [3] presented his theory that rupture will originate in the minimum film thickness region and remains constant in divergent region followed by swift[8] & Stieber [9] but not discussed about film reformation. The theory was not fulfilling mass continuity condition which is also called as half Sommerfeld condition. Experimental occurrence of sub cavity pressure loop was observed by Hopkins (6) in 1957, Bretherton (7), Taylor (8) in 1960, and Coyne and Elrod (9), in 1970 which was neglected by Gumbel, swift and Stieber. Separation would occur between film rupture when derivative of velocity in y direction is equal to zero but due to this secondary flow generated causing flow reversal region in which dissolved gases can congregate.

For running journal bearing system properly eccentricity ( $e$ ) should be minimum for keeping optimum equilibrium state throughout the operation. If direct contact occurs between the shaft and bearing, generation of high temperature take place which degrade the mechanical performance. [10] Failure of HDB may occur due to many reasons such as high temperature of journal bearing causing sintering, wear out journal bearing, wear particles in lubricants, severe vibration, oil whirl and may more. Researcher tries to optimize parameters that lead to minimize the failure of journal bearing. A number of failure models are proposed by authors and discussed[11]. Through the use of composite material for journal bearing and by mixing additives[12] [13] [14] in fluids[15]–[19] leads of reduce friction and wear. By using these different methods operating parameters will improvise with more stability

Hsu et al (2003) investigated the combined effect of couple stresses and surface roughness. Results show that with longitudinal roughness, load carrying capacity was improved with decrease in attitude angle and friction while with transverse roughness behaves opposite in nature through variation in operating parameters with multiphase flow. Optimised set was presented by several author with attitude angle, eccentricity, operating speed and load for better functionality at worse conditions [21].

Pressure in hydrodynamic bearing is always varying with operating parameters. It was found that the pressure distribution could be negative [22] in oil lubricated bearing due to cavitation which causes metal to metal contact resulting wear. As technology advances in the field of computer takes place and use of computation fluid dynamics (CFD) program to solve cavitation, it eases the method of computation which is based on lubrication theory to analyse flow in HDJB [23], [24]. CFD approaches were also proposed to do the same [25]. As shaft rotates during which if whirling occur causing cavitation due to pressure disturbance was demonstrated. Fluid film pressure and load capacity can be optimised with the use of couple stress fluid (CSF). Also optimized set of journal speed and couple stress fluid shows better results with cavitated finite journal bearing (FJB)[26]. Effect of cavitation and journal whirl on the static and dynamic characteristic of journal bearing was evaluated through CFD for single and 2 phase flow models. Sun et al [27]studied the Stability of journal bearing which was affected due to whirl frequency.

As fluids are used in HDB where flow should be laminar or turbulent which affect the performance characteristics that can be studied through use of CFD to predict the outcome before the actual trial run. Also fluid properties affect the bearing

performance and helps in reducing temperature during the runs[28]. There are several models presented to solve the CFD problem that can give more accurate solution at faster rate. There are different types of cavitation i.e. gaseous, Pseudo and vapour cavitation occurred in HDB for which models were compared with its limitation to evaluate the performance parameter. The size of nuclei that develop due to pressure difference in the flow regime aid cavitation. [5] He experimentally shows that at high rotational speed and low lubricant supply pressure, bearing performance was affected due to cavitation. Most of the literature study show that load carrying capacity decreases at higher speed due to large cavitation area. [29] Reported that with variation in film thickness and oil supply pressure, negative effect of cavitation can be reduced. Stiffness of HDJB was calculated with cavitation was considered which is of  $10^7$  to  $10^8$  N/m. Zhang (2015) presented relationship between clearance, different L/D ratio with different rotational speed. Author presented a method for evaluating the stiffness coefficient of hydrodynamic plain journal bearings lubricated by water. Results show that how load carrying capacity and stiffness coefficient affected with change in diameter. For better load carrying capacity, hydrodynamic bearings can externally pressurised with the help of pumps [31]. Also with changes in bush structure, LCC can be increased[32].

For getting accurate results at faster rate new algorithm were also developed to reduce the time of getting result through use of high speed system and with new method of designing the setup. Schlegel [33] showcase the lower usage of CPU through “lower dimension” approach for optimization. Also multiphysics simulation was performed to check stability for all loading condition, response of the rotor to unbalanced loads and effect of friction losses of hydrodynamic bearings. Alakshramsing [34] uses the mass conservation method to reduce the processing time for convergence in finite element analysis. Literature shows that attempt was made to improve the static and dynamic characteristics of journal bearing by varying the performance dependent parameters but yet detailed studies do not seem to have been studied sufficiently.

The objective of this study is to apply CFD prediction model to investigate the effect of variation in L/D ratio, eccentricity ratio and rpm on the evolution and termination of pressure variation causing failure of journal bearing due to cavitation at the middle ring circumferentially.

## 2.0 Theoretical analysis

### 2.1 Journal bearing

Journal Bearing is used to cater the high load carrying capacity with the use of different lubricant. These lubricants have different properties as per the use. In this arrangement the bearing is stationary and journal is rotating and when there is a deviation from the bearing centre, pressure difference is generated to bear the vertical load. The distance between the journal and bearing is eccentricity ( $e$ ) and the angle by which the journal deviates from its vertical called the attitude angle ( $\Phi$ ). At the starting, there is a contact between the journal and bearing with eccentricity between them which is maximum. As the journal commences rotation, it tries to minimize the eccentricity while bearing the load. There are several parameters which try to deviate the journal from the bearing center which are load ( $L$ ), speed ( $N$ ), L/D ratio, relative

clearance ( $\Psi$ ) and temperature. So bearing model with different L/D ratio, speed and temperature to be studied which effect the minimum fluid film thickness. The maximum relative ratio varies with relative clearance when  $R$  is fixed. To find the failure due to cavitation when the load, speed and temperature is varied by keeping the diameter of 50 mm. with reference to bearing design, relative clearance, L/D ratio and speed are listed in table 1 and 2 simulations are modelled to study the cavitation. To find the reason behind this, a CFD model was created in Fluent 17.2 on which iteration was done by varying the L/d ratio, speed and eccentricity.

### 2.2 Journal bearing modelling

Schematic of journal bearing was shown in fig 1 with coordinate system. There are several parameters which affect the proper functionality of HDB such as load, diameter, relative clearance, L/D ratio and rotational speed. Failure due to instability in both the region causes cavitation which needs to be studied as it is affected by load, rpm and relative clearance etc. For this model with different relative clearance, speed and L/D ratio was studied which effects the minimum fluid film thickness which is given by  $h_{min} = R\Psi(1-\epsilon)$ . In this study, determination of influence of  $\psi$ , L/D ratio and  $N$  on failure due to cavitation for which the diameter is fixed at 50 mm. Relative clearance ( $\psi$ ) ranges between 0.06% to 0.2% and the L/D ratio varied from 0.5 to 2 [30] with speed range from 10 to 1000 rpm with eccentricity ratio( $\epsilon$ ) between 0.4 to 0.9. [35]

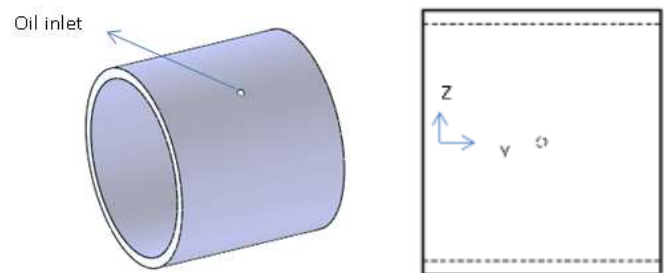


Fig 1: Diagram of journal bearing

Table.1: Values of design parameters

<b>D (MM)</b>	50
<b>Ψ (%)</b>	0.06,0.08,0.1,0.12,0.14,0.16,0.18,0.2
<b>L/D</b>	0.5,1,2
<b>N(r/min)</b>	10,100,1000
$\epsilon$	0.4-0.9

The flow is considered isothermal, steady and incompressible, with zero gravitational or other external body forces.

### 2.3 Governing equation

For solving all fluid problem, Fluent solves conservation equation for mass and momentum[36]. The continuity equation to solve the fluid flow problem can be written as

$$\frac{\partial \rho}{\partial t} + \nabla(\rho \vec{v}) = 0$$

Where  $\rho$  and  $\vec{v}$  are the fluid density and fluid velocity vector and is valid for compressible and incompressible flow. P can be calculated from the one dimensional Reynolds equation but value of  $\Psi$  &  $\epsilon$  depends on the configuration, loading condition and lubricant used. The momentum conservation equation in an inertial (non- accelerating) reference frame is:

$$\frac{\partial}{\partial t} (\rho \vec{v}) + \nabla (\rho \vec{v} \vec{v}) = -\nabla p + \nabla(\vec{\tau}) + \rho \vec{g} + \vec{F}$$

Where p is the static pressure,  $\vec{\tau}$  is the stress tensor and  $\rho \vec{v}$  and  $\vec{F}$  are the gravitational body force and external body force, respectively. The stress tensor ( $\vec{\tau}$ ) is given by

$$\vec{\tau} = \mu [(\nabla \vec{v} + \nabla \vec{v}^T) - \left(\frac{2}{3}\right) \nabla \cdot \vec{v} \mathbf{I}]$$

Where  $\mu$  is the fluid viscosity, I is the unit tensor and the second term on the right hand side is the effect of volume dilation.

### 2.4 Assumption and boundary condition

The flow model and boundary condition for the journal bearing created in Design modeller which was used for simulation purpose. The flow which was taken place in the journal bearing was considered as isothermal, steady and incompressible with no gravitational force or other external body force. The viscosity model was set to laminar model as Reynolds's no = 1412.89 (D = 50 mm and N = 1000 rpm).

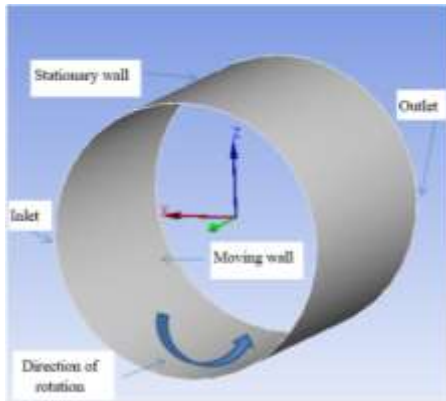


Fig 2: Flow model and boundary condition

Film clearance was taken as inlet on one side and outlet on the other side of the model. Pressure at inlet and outlet was taken as 0 Pa (gauge pressure). Outer wall was set as stationary wall and inlet wall was set as moving wall with no-slip condition. SIMPLEC model was selected for velocity pressure coupling for converged solution as compared to SIMPLE[37]

### 3.0 CFD model analysis

For evaluating pressure on hydrodynamic bearing, simulation were done on Ansys (CFD)- 17.2 version was used. While meshing the geometry, quad elements have been used with 10 elements longitudinally with soft behaviour and 1.20 growth rate with no bias as shown in fig 2a. Also 360 divisions are made circumferentially with mapped mesh on. The aspect ratio got after meshing was 143 – 155. For normal analysis the suggested aspect ratio as per user manual should be within 200. To avoid negative influence of the large aspect ratio, double precision calculation is employed as per the manual of

Ansys. The solver selected is pressure based and the algorithm used is SIMPLEC for coupling the velocity and pressure. The scheme for momentum equation is second order upwind discretisation scheme was used. The convergence tolerance used is  $10^6$  for all residual terms. The calculation was terminated as the force remains unchanged.

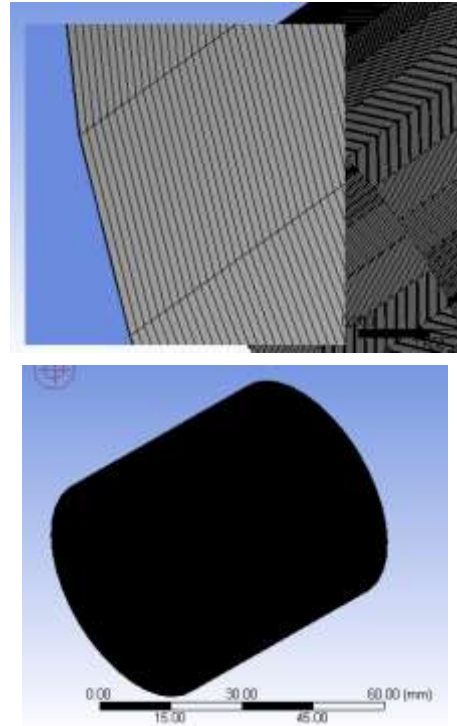


Fig.2a Meshed journal bearing model

### 3.1 Methodology validation

To validate the model used in our case, for different L/D ratio pressure was calculated on the middle ring of the journal bearing by simulating in fluent i.e. D = 80 mm, L/D = 1,  $\psi = 0.1\%$ , N = 3000 r/min &  $\epsilon = 0.6$  are compared with results obtained by Xiuli et. al.[30]. From the contour i.e. Fig 3, the pressure achieved by the author matches almost with the result as shown in his paper and showing the pressure build up in the convergent region and occurrence of cavitation in the divergent film.

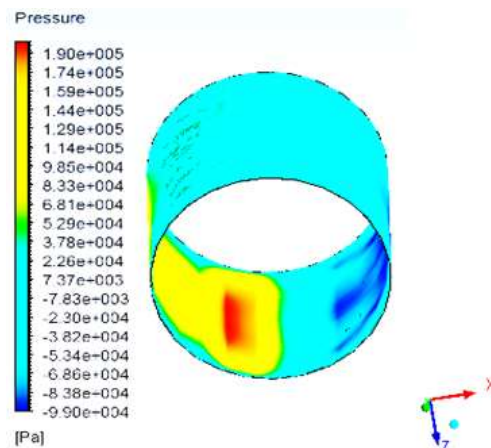


Fig. 3: Contour of static pressure(Pa) for turbulent model

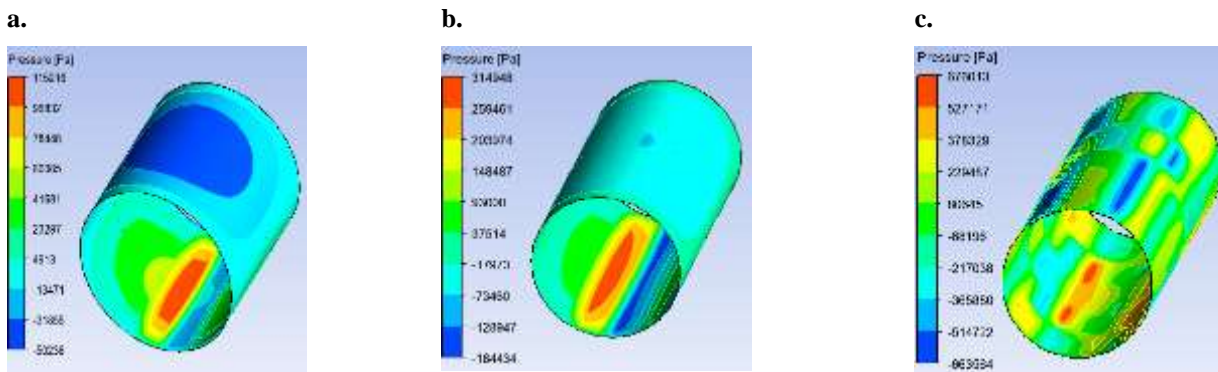


Fig 4: Dimensionless pressure ( $P = p\psi^2/\mu\omega$ ) distribution at  $z = L/2$

Figure 4 shows pressure contour in convergent and divergent region for different L/D ratio (0.5, 1 & 2) with relative clearance and (0.0006) & eccentricity ratio (0.05). To study the performance of HDB in terms of LCC and compare the variation in pressure vs. theta, simulation were performed with the input parameters (e, rpm & L/D ratio) for a laminar model based on Reynolds no. From the contour the maximum pressure achieved was 676013 Pa for L/D = 2 as compared to L/D = 0.5, 1 as 115216, 314948 Pa. Also the load carrying capacity increases with increase in L/D ratio but the pressure distribution is more stable in fig 4a and 4b as compared with 4c, it is more disturbing due to long length of bearing or insufficient lubricant supply. Also the divergent region is more thinning with increase in L/D ratio at same rpm

#### 4.0 Result and discussion

Simulations were performed by varying eccentricity for different speed & L/D ratio on CFD as per Table 1 & 2. Graphs were plotted between dimensionless pressure and theta to study the failure due to cavitation in hydrodynamic bearings.

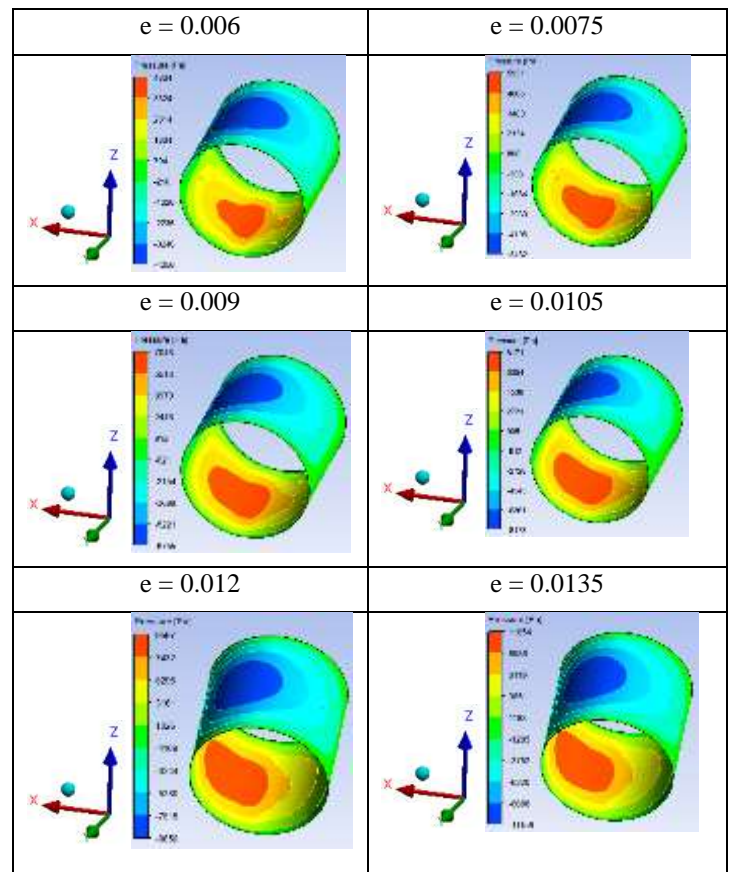
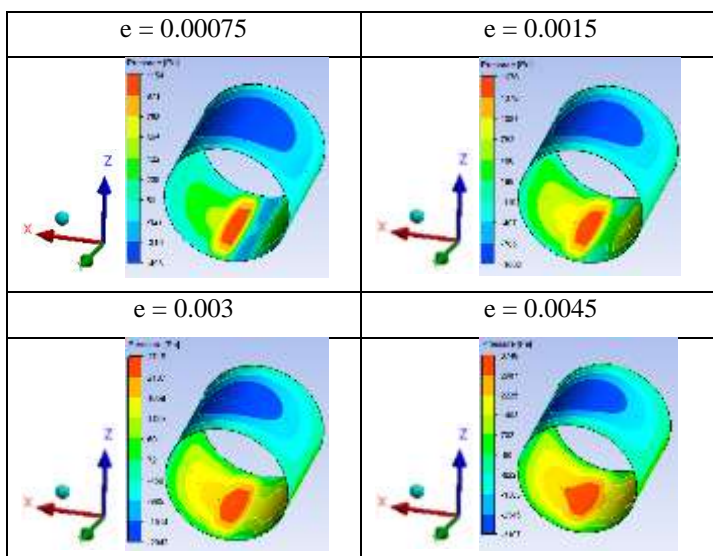
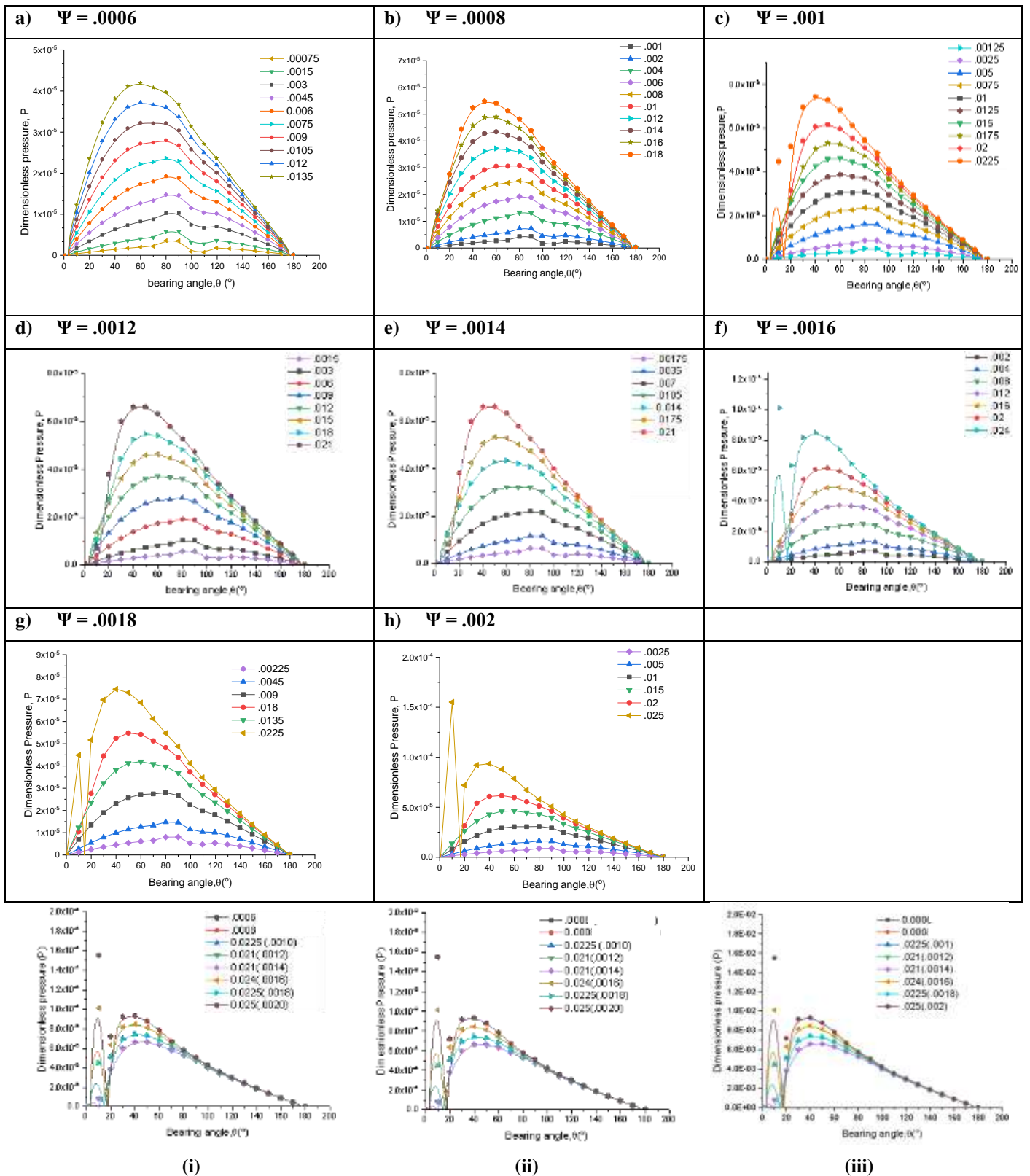


Fig 5: Pressure contours with different eccentricity for L/D = 0.5 at 10 r/min with different eccentricity (e)

Simulated results of pressure contour were plotted for positive and negative region on the fluid film in convergent and divergent region of HDB at 10 rpm by varying the eccentricity & L/D = 0.5 were shown in Fig. 5. From the contour it can be clearly seen that the region of positive pressure in convergent zone increase with increase in eccentricity at same rpm. Also the maximum pressure attained during the simulation was 11054 Pa.





**Fig 6** Dimensionless pressure vs. Bearing angle for  $L/D = 0.5$   
 Graphical plot were shown in figure 6 between Dimensionless pressure vs. theta for  $L/D = 0.5$  at 10 rpm with varying relative clearance ( $\Psi$ ). It shows that the pressure increases as the eccentricity value increases. The -ve pressure region was occurred at  $180^\circ$  to  $360^\circ$  in most of the cases i.e. divergent region. For  $\Psi = 0.0006$  &  $0.0008$ , cavitation occur at  $180^\circ$  for all eccentricity but when  $\Psi = 0.001$  &  $e = 0.0225$  due to load, the fluid film rupture at start ( $0^\circ$ ) and end at  $19^\circ$  causing  
 Copyrights @Kalahari Journals

cavitation in the convergent region but settle to positive pressure due to higher pressure build up. The outcome of these plot indicate that for short journal bearing the pressure in divergent zone was negative but in few cases with higher eccentricity values the cavitation occur in convergent region between  $0^\circ - 20^\circ$  due to minimum fluid film thickness at the initial start as speed was low and load was high but after  $20^\circ$  regain +ve pressure due to high pressure build-up. It was also observe from the plot that form 6 (a -h) that as  $\Psi$  increases,

the dimensionless pressure increases leading to higher load carrying capacity of HDB.

**Fig 6** Cavitation Plot at various  $\epsilon$  ( $\epsilon$ ) with different rpm and  $L/D = 0.5$  at (i) 10 rpm (ii) 100 rpm (iii) 1000

It was found that with increase in rpm for  $L/D = 0.5$  mm, occurrence of cavitation was not found at first two eccentricity values but as the rpm increases the cavitation was found at same values of eccentricity. The hydrodynamic lubrication was achieved initially but when the rpm increases with eccentricity instability were occurred due to which sufficient amount of lubricant was not maintained results in cavitation. Also it was found that the maximum pressure was  $1.6 * e^{-4}$  Pa.

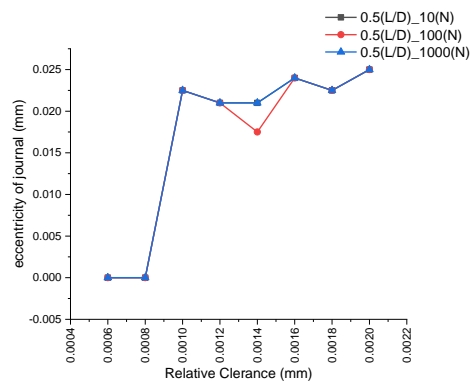


**Fig 7:** Relative clearance vs. eccentricity of journal (occurrence of cavitation) for different L/D ratio

As we found that when the bearing starts running, there was no cavitation for all the cases i.e.  $N = 10, 100 \& 1000$  RPM. With increase in speed & eccentricity, results shows that the maximum value of eccentricity is 0.025 mm for all the three cases while maintaining no contact between journal and shaft. As the relative clearance increases with speed, load carrying capacity also increases upto a certain extent after which cavitation occurs due to insufficient supply of fluid causing pressure difference region.

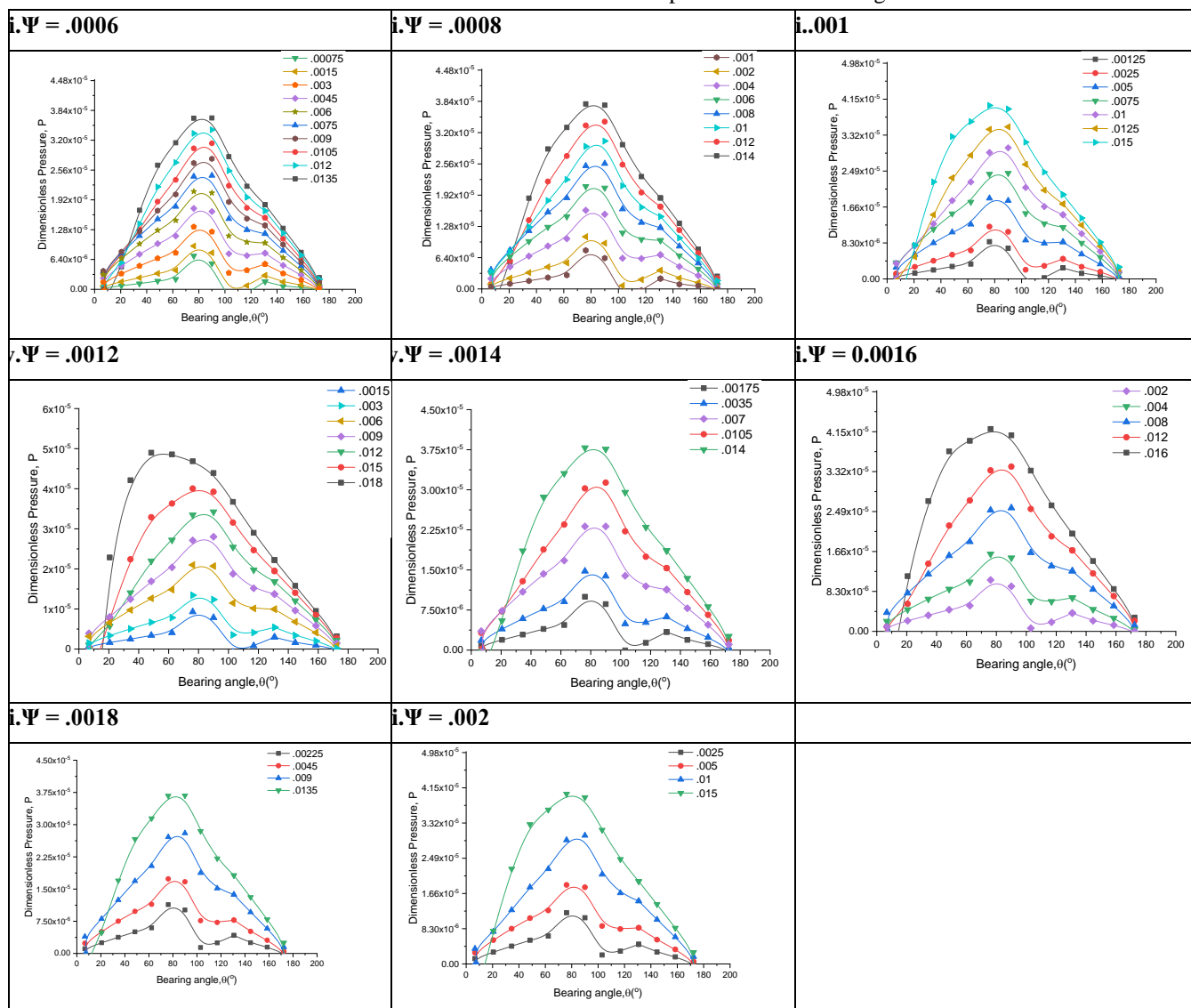


**Fig 8** Dimensionless pressure vs. Bearing angle for different values of  $L/D = 1$

Figure 8 represents plot between pressure vs. theta (degree) for  $L/S = 1$  at 10 rpm. The peak pressure at different eccentricity ratio increases with increase in  $L/D$  ratio but with a little disturbance as in comparison to  $L/D = 0.5$ , occurrence of film rupture at start commences early in case of  $L/D$  at same rpm but peak pressure drops from  $4e^{-5}$  to  $-3.80e^{-5}$ . In figure 8 (i) positive pressure build-up at start of convergent region between  $100^{\circ}$  to  $120^{\circ}$ , the cavitation occur but regain to positive pressure region. It is observed from the plot that for initial run at different  $\Psi$ , the occurrence of negative pressure between  $100^{\circ} - 120^{\circ}$  diminishes in other cases i.e. 8 (v – viii). Simulation shows that as the eccentricity ration increases, the peak pressure increases till 8 (i – iv) but after

this drop in pressure was observed and then again rise between 8 (vi – viii) which may be due to larger  $L/D$  ratio with more disturbance in pressure plot. Also it was seen that at occurrence of negative pressure at start achieved at lower value of  $\Psi$  that also due to larger  $L/D$  ration and lower speed. By keeping the same relative clearance & speed with change in  $L/D$  ratio of 1, result show that cavitation occur at earlier stage when compared with the results of  $L/D = 0.5$ . It is clear from the results that with increase in the length of the hydrodynamic bearing with eccentricity pressure difference between convergent and divergent region increases results in cavitation.

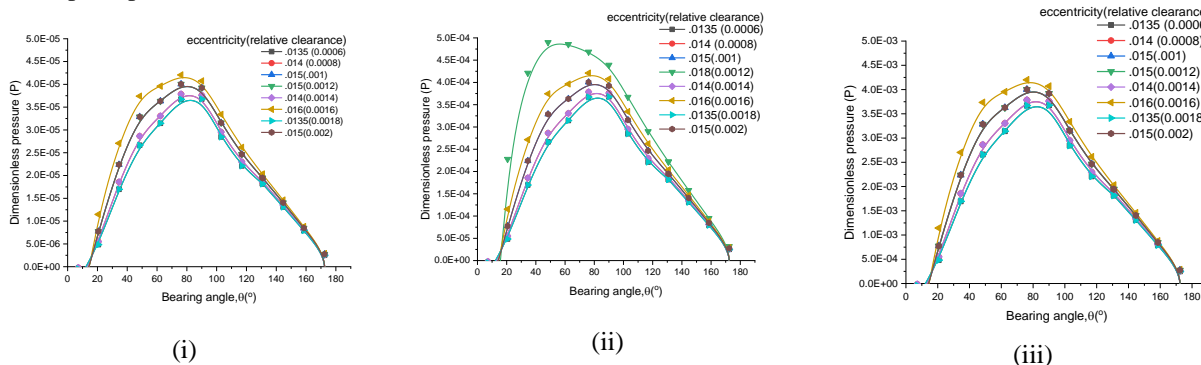


**Fig 8a.** Cavitation Plot at various  $e$  ( $\epsilon$ ) with different rpm and  $L/D = 1$  at (i) 10 rpm (ii) 100 rpm (iii) 1000 rpm

From fig 8a, the maximum pressure acquired during the simulation at different rpm with eccentricities is  $4 * e^{-5}$  which is at the lowest speed. The occurrence of negative pressure at start with different  $\Psi$  seen between  $0 - 200$  with positive pressure build up with variation in rpm. Also with increase in rpm, the peak pressure also rises for  $L/D = 1$  which proportionally increases the load carrying capacity but lower than that of  $L/D = 0.5$  fig 6a (i-viii) & 8a (i-viii).

up and journal bearing was not able to regain to positive pressure region i.e. convergent region if it occur at the start of the run. The performance of bearing with different  $L/D$  ratio i.e. 0.5 & 1 was good with better load carrying capacity.

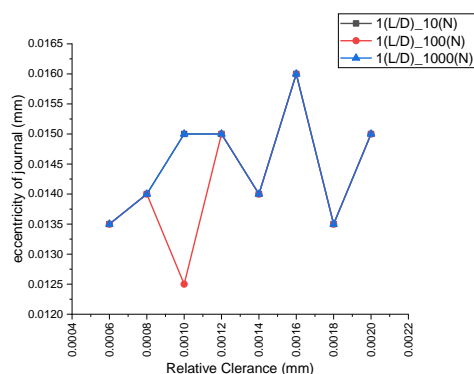


**Fig 9:** comparison of relative clearance and occurrence of cavitation for different speed

Result shows that by varying the speed of rotation and keeping the same relative clearance, occurrence of cavitation is same in each case when  $L/D$  ratio was 1. A slight variation is seen at  $\Psi = 0.0010$ .

Simulation was also performed to see the variation in pressure distribution at  $N = 10$  RPM with  $L/D$  ratio = 2 at different  $\Psi$  and graph were plotted between Dimensionless pressure and theta but pressure distribution was troublesome in comparison to  $L/D = 0.5$  & 1 causing cavitation. This may be due to long length of the bearing which gets more surface area compared to previous cases and also due to insufficient pressure build

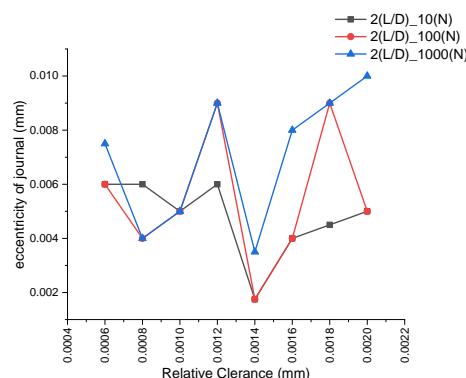


**Fig 12:** Comparisons between relative clearance and occurrence of cavitation for  $L/D = 2$

With same eccentricity values and increasing the speed to 1000 rpm for  $L/D = 2$  shown in figure 12. Result shows that failure for  $\psi = .0006$  and  $.008$ . For relative clearance of 0.001, 0.0012 and so on, bearing facing difficulty at start and after certain cycle it achieve stability. It was also found in few cases that after attaining stability, unstability occurs with higher relative clearance ( $\psi = .0014$ ) and while in few completely positive pressure was maintained ( $\psi = .0016, .0018, .002$ ).

### 5.0 Conclusion

This study investigates the failure phenomena due to cavitation in hydrodynamic bearing. The parameters were chosen are the relative clearance, speed,  $L/D$  ratio with fixed

diameter of bearing. Fluent 17.2 was used for simulation and graphs were plotted between dimensionless pressure and bearing angle for different eccentricity ratio, speed and L/D ratio. With the help of these graph, conclusion were made which are:

- a. Result shows that the pressure range achieved for 50 mm journal bearing at different speed, L/D ratio and eccentricity was  $10^3$  to  $10^{11}$  Pa.
- b. Hydrodynamic equilibrium was seen at 0.006 and 0.008 relative clearance for L/D = 0.5 but not for L/D = 1 and 2 as it increases with rpm. In L/D = 2 maintain stability of journal bearing during the run was difficult but maximum pressure achieved.
- c. Occurrence of cavitation at earlier stage was also found as eccentricity and L/D ratio increases with increase in speed. This may be due to increase in length of bearing and it is recommended that precaution is be taken by designer for selecting the proper ratio between rpm, L/D ratio and lubricant used for large L/D ratio.
- d. At minimum and maximum eccentricity for L/D = 2 cavitation was seen but in-between the run was smooth with highest pressure attainment that may be due to sufficient amount of lubricant supply between the convergent and divergent region as journal stabilises.
- e. Load carrying capacity of HJB increases with increases in L/D ratio but achieving stability was difficult at different eccentricity and rpm. This can be achieved with external pressurised fluid supply.

## References

- [1] M. J. Braun and R. C. Hendricks, "An experimental investigation of the vaporous/gaseous cavity characteristics of an eccentric journal bearing.," no. December 2013, pp. 37–41, 1982.
- [2] M. Zupanc, Ž. Pandur, T. Stepišnik Perdih, D. Stopar, M. Petkovšek, and M. Dular, "Effects of cavitation on different microorganisms: The current understanding of the mechanisms taking place behind the phenomenon. A review and proposals for further research," *Ultrason. Sonochem.*, vol. 57, pp. 147–165, 2019.
- [3] D. Dowson, C. M. Taylor, C. I. N. Bearings, D. Dowson, and C. M. Taylor, "Cavitation in bearings," *Annu. Rev. Fluid Mech.*, pp. 35–66, 1979.
- [4] C. C. Wang and C. L. He, "Numerical study of a hydrodynamic journal bearing with herringbone grooves for oil leakage reduction," *Proc. Inst. Mech. Eng. Part J J. Eng. Tribol.*, vol. 233, no. 3, pp. 439–446, 2019.
- [5] M. J. Braun and W. M. Hannon, "Cavitation formation and modelling for fluid film bearings: a review," *Proc. Inst. Mech. Eng. Part J J. Eng.*, 2010.
- [6] G. W. Stachowiak and A. W. Batchelor, *Engineering tribology*. Butterworth-Heinemann, 1993.
- [7] D. Dowson, "Elastohydrodynamic and micro-elastohydrodynamic lubrication," *Wear*, vol. 190, no. 2, pp. 125–138, 1995.
- [8] H. W. Swift, "The Stability of Lubricating Films in Journal Bearing," *Proc. Inst. Civ. Eng.*, vol. 233, pp. 267–288, 1932.
- [9] W. Stieber, "Dasschwimmlager: Hydrodynamische Theorie des Gleitlagers," *V.D.I. Verlag GMBH, Berlin*, p. 106.p, 1933.
- [10] Y. He, Z. Zhao, T. Luo, X. Lu, and J. Luo, "Failure analysis of journal bearing used in turboset of a power plant," *Mater. Des.*, vol. 52, pp. 923–931, 2013.
- [11] Youyun Zhang, "Encyclopedia of Tribology," *Encycl. Tribol.*, 2013.
- [12] D. X. Peng, C. H. Chen, Y. Kang, Y. P. Chang, and S. Y. Chang, "Size effects of SiO<sub>2</sub> nanoparticles as oil additives on tribology of lubricant," *Ind. Lubr. Tribol.*, vol. 62, no. 2, pp. 111–120, 2010.
- [13] M. M. Khonsari and E. R. Booser, "Effect of contamination on the performance of hydrodynamic bearings," *Proc. Inst. Mech. Eng. Part J J. Eng. Tribol.*, vol. 220, no. 5, pp. 419–428, 2006.
- [14] S. B. Chikalthankar, V. M. Nandedkar, and P. V. Jawale, "Comparative Study of Bearing Materials and Failure of Plain Bearings," *Int. J. Eng. Res. Technol.*, vol. 3, no. 2, pp. 2402–2406, 2014.
- [15] J. Jia, J. Lu, H. Zhou, and J. Chen, "Tribological behavior of Ni-based composite under distilled water lubrication," *Mater. Sci. Eng. A*, vol. 381, no. 1–2, pp. 80–85, 2004.
- [16] J. H. Jia, J. M. Chen, H. Di Zhou, J. B. Wang, and H. Zhou, "Friction and wear properties of bronze-graphite composite under water lubrication," *Tribol. Int.*, vol. 37, no. 5, pp. 423–429, 2004.
- [17] H. Unal and A. Mimaroglu, "Friction and wear characteristics of PEEK and its composite under water lubrication," *J. Reinf. Plast. Compos.*, vol. 25, no. 16, pp. 1659–1667, 2006.
- [18] W. Huang, Y. Xu, Y. Zheng, and X. Wang, "The tribological performance of Ti(C,N)-based cermet sliding against Si<sub>3</sub>N<sub>4</sub> in water," *Wear*, vol. 270, no. 9–10, pp. 682–687, 2011.
- [19] J. Wang, F. Yan, and Q. Xue, "Tribological behavior of PTFE sliding against steel in sea water," *Wear*, vol. 267, no. 9–10, pp. 1634–1641, 2009.
- [20] C. H. Hsu, J. R. Lin, and H. L. Chiang, "Combined effects of couple stresses and surface roughness on the lubrication of short journal bearings," *Ind. Lubr. Tribol.*, vol. 55, no. 5, pp. 233–243, 2003.
- [21] D. Y. Dhande and D. W. Pande, "Multiphase flow analysis of hydrodynamic journal bearing using CFD coupled Fluid Structure Interaction considering cavitation," *J. King Saud Univ. - Eng. Sci.*, vol. 30, no. 4, pp. 345–354, 2018.
- [22] T. Someya, "On the development of negative pressure in oil film and the characteristics of journal bearing," *Meccanica*, vol. 38, no. 6, pp. 643–658, 2003.
- [23] G. C. Buscaglia, I. Ciuperca, and M. Jai, "The effect of periodic textures on the static characteristics of thrust bearings," *J. Tribol.*, vol. 127, no. 4, pp. 899–902, 2005.
- [24] V. D'Agostino and A. Senatore, "Analytical solution for two-dimensional Reynolds equation for porous journal bearings," *Ind. Lubr. Tribol.*, vol. 58, no. 2, pp. 110–117,



2006.

- [25] B. Manshoor, M. Jaat, Z. Izzuddin, and K. Amir, "CFD analysis of thin film lubricated journal bearing," *Procedia Eng.*, vol. 68, pp. 56–62, 2013.
- [26] M. A. Mahdi, A. W. Hussain, and H. H. Hadwan, "Investigation of cavitation in a finite journal bearing considering the journal speed and couple stress fluids effects," *Tribol. Ind.*, vol. 40, no. 4, pp. 670–680, 2018.
- [27] D. Sun, S. Li, C. Fei, Y. Ai, and R. P. Liem, "Investigation of the effect of cavitation and journal whirl on static and dynamic characteristics of journal bearing," *J. Mech. Sci. Technol.*, vol. 33, no. 1, pp. 77–86, 2019.
- [28] S. Kumar, V. Kumar, and A. K. Singh, "Influence of lubricants on the performance of journal bearings—a review," *Tribol. - Mater. Surfaces Interfaces*, vol. 14, no. 2, pp. 67–78, 2020.
- [29] Y. Song, X. Ren, C. W. Gu, and X. S. Li, "Experimental and numerical studies of cavitation effects in a tapered land thrust bearing," *J. Tribol.*, vol. 137, no. 1, 2015.
- [30] X. Zhang, Z. Yin, G. Gao, and Z. Li, "Tribology International Determination of stiffness coefficients of hydrodynamic water-lubricated plain journal bearings," *Tribology Int.*, vol. 85, pp. 37–47, 2015.
- [31] "Institution of Mechanical Engineers," in *Proceedings of the Institution of Mechanical Engineers, Conference Proceedings*, 2015.
- [32] G. Gengyuan, Y. Zhongwei, J. Dan, and Z. Xiuli, "CFD analysis of load-carrying capacity of hydrodynamic lubrication on a water-lubricated journal bearing," *Ind. Lubr. Tribol.*, vol. 67, no. 1, pp. 30–37, 2015.
- [33] F. Schlegel, "Predicting Cavitation in Journal Bearings," *COMSOL*, 2015. [Online]. Available: <https://www.comsol.com/blogs/predicting-cavitation-in-journal-bearings>.
- [34] S. Alakhramsing, R. van Ostayen, and R. Eling, "Thermo-hydrodynamic analysis of a plain journal bearing on the basis of a new mass conserving cavitation algorithm," *mdpi*, vol. 3, no. 2, pp. 256–280, 2015.
- [35] G. Gao, Z. Yin, D. Jiang, and X. Zhang, "Numerical analysis of plain journal bearing under hydrodynamic lubrication by water," *Tribol. Int.*, vol. 75, no. February 2020, pp. 31–38, 2014.
- [36] F. 6.3, *Text Command List*, no. September. Fluent, 2006.
- [37] A. Fluent, "ANSYS FLUENT, Version 14.0: User Manual. ANSYS, Inc.: Canonsburg, USA," *ANSYS Inc., USA*, vol. 15317, no. November, pp. 724–746, 2013.